DOI: 10.21062/mft.2024.069 http://www.journalmt.com

Experimental Identification of Gear Mesh Stiffness and Verification by Theoretical Models

Jan Flek (0000-0003-4495-1206)[1], Tomas Karas (0009-0005-7202-6036)[1], Martin Dub (0000-0002-4027-0465)[1], Frantisek Lopot (0000-0001-5731-6784)[1], Vit Ripa (0000-0002-9701-8287)[1], Josef Kolar (0000-0002-4648-6515)[2]
[1]Department of Designing and Machine Components, Faculty of Mechanical Engineering, Czech Technical University in Prague, Technicka 4, Prague 6, 160 00 Dejvice. Czech Republic. E-mail: jan.flek@fs.cvut.cz, tomas.karas@fs.cvut.cz, martin.dub@fs.cvut.cz, frantisek.lopot@fs.cvut.cz, vit.ripa@fs.cvut.cz
[2]Department of Automotive, Combustion Engine and Railway Engineering, Faculty of Mechanical Engineering, Czech Technical University in Prague, Technická 4, Prague 6, 160 00 Dejvice. Czech Republic. E-mail: josef.kolar@fs.cvut.cz

When analyzing the natural frequencies of a gear mechanism, it's crucial to consider the mesh stiffness, which is influenced by the number of teeth in the mesh. Mesh stiffness behaves as an internal excitation source for the dynamic system, affecting the resulting frequency spectrum. This paper presents an experimental determination of gear mesh stiffness supported by analytical-simulation models of mesh stiffness, outlining common modeling methods and detailing the experimental setup and test specimens. The obtained data are then compared with simulation models of mesh stiffness, discussing the significance of this comparison and emphasizing the role of experimental data in validating and refining existing models of mesh stiffness. The experimental measurement of mesh stiffness described here emerges as a valuable tool for accurately representing mesh stiffness during engagement.

Keywords: Spur Gears, Dynamic excitation, Gear Mesh Stiffness, Experimental identification, Theoretical Models

1 Introduction

When designing gearbox systems, it is of paramount importance to take into account the dynamic properties of gears. Optimal gear geometry can exert a favorable influence on the dynamic response of the system, which mani-fests itself through observable changes in the frequency spectrum of the investigated dynamic system. Furthermore, appropriately designed gear geometry has the potential to significantly reduce noise emissions. The articles discuss determining the optimal gearing geometry are [1, 2]. The frequency spectrum of gears predominantly reflects the effect of internal excitation caused by mesh stiffness, a parameter that exhibits variation during meshing, thereby significantly impacting the torsional dynamic processes of the gear system. The significance of dynamic calculations and the determination of vibration states are addressed in the articles [3-5], which focuses on the analytical and experimental investigation of vibrations in a system of interconnec-ted bodies. The authors highlight the impact of vibrations on the longevity of components and the propagation of undesired noise.

Multiple approaches are available to visualize, simulate, and calculate mesh stiffness behavior in gearing. Among the analytical calculations available, the method that computes the deformation energy of individual gear teeth to determine mesh stiffness is likely the most accurate, [6-10, 12]. This method allows consideration of several additional calculation conditions, such as involute tooth side defects and modeling of root cracks, both of which can significantly impact mesh stiffness, [7-9, 12]. Incorporating the effect of lubrication between functio-nal tooth surfaces in the analytical model based on deformation energy can further increase accuracy and provide a more precise approximation of the actual stiffness behavior of the gear train, [10].

In terms of modeling gear stiffness, KISSsoft calculation software offers a commercially available solution. This software permits gear geometries to be designed, and stiffness can be determined based on the specific geo-metry. The calculation model is a modified version of the gear stiffness model based on deformation energy and is founded on Weber's theory, [13]. Nevertheless, the calculation is less detailed since it does not allow the precise description of a tooth's real geometry with defects or cracks at the dedendum of the tooth.

With modern advancements, it is possible to determine mesh stiffness accurately using finite element method simulation. This technique enables precise determination of the stiffness of each gear. Nevertheless, this method's efficacy is heavily reliant on the computational model's processing quality and the specified boundary conditions. Although the finite element method offers high precision in determining mesh

stiffness, it is not necessarily a straightforward verification tool for analytical methods. The finite element method is used in these publications to determine the mesh stiffness of gearing, [11, 14-16].

Experimental measurement is the final method discussed in this paper for determining gear engagement stiff-ness. While it is the last approach mentioned, experimental measurement is the only method that can serve as a verification tool for evaluating the stiffness course obtained from analytical-simulation methods. From the per-spective of stiffness determination accuracy, experimental measurement is the optimal choice. However, the high cost of experimental habitats presents a significant drawback to this approach, resulting in few verification expe-riments being performed by researchers. In their contributions, authors Raghuwanshi, N. K., and Parey, A. used deformation measurements with a camera (digital image correlation) to determine the mesh stiffness course, [18]. In their further research, they dealt with the experimental verification of mesh stiffness due to the photoelasticity method, [17], experimental modal analysis, [20], and the laser displacement sensor method, [19]. Experimental mesh stiffness measurements were also performed by authors Karpat, F., Yuce, C. and Doğan, O., who determined the stiffness of single tooth of involute spur gear by means of loading and measuring the deformation displacement of the tooth, [21]. Other authors Kong, Y. et al. attempted to obtain data based on experimental measurements of mesh stiffness involving the dynamic response of the gear mechanism, [22]. The primary focus of this paper is to determine the actual mesh stiffness of gearing. To achieve this goal, the article introduces a range of computational models that describe gear engagement stiffness. In addition, the paper highlights the potential for experimental measurements to provide more realistic mesh stiffness data. The experimental rig function is described in detail, including the methodology used to perform the measurements and the interpretation of the initial data. In the discussion section, the results obtained from analytical simulation models, such as the deformation model, KISS-soft calculation model, and FEM model, are presented for mutual comparison. The suitability and applicability of these stiffness modeling methods are evaluated based on the results obtained. Additionally, the limitations of ana-lytical methods are emphasized, highlighting the need for experimental measurements to validate and improve the accuracy of stiffness models. Overall, this paper provides a comprehensive overview of the methods used to de-termine the mesh stiffness of gearing, including the use of computational models and experimental measurements. By comparing the results obtained from different modeling methods, the paper offers insights into the strengths and limitations of each approach.

2 Analytical-Simulation Models of Mesh Stiffness

This chapter outlines three distinct options for modeling the course of mesh stiffness: deformation energy, KISSsoft model, and FEM model. The stiffness of the meshing process is dependent on the geometrical and mate-rial properties of the gear teeth and is time-varying due to the gears' engagement. The relationship between the load on the tooth and its deformation can be represented using the tooth's cantilever beam model with a varying cross-section, with the force acting in the direction of the line of action.

In this case of a spur gear with straight teeth, the engagement of one pair of teeth and two pairs of teeth alterna-tes, resulting in a fluctuation of the mesh stiffness. The changes in the stiffness course during gear engagement can be modeled using any of the three approaches described in this chapter. However, each method has its advantages and limitations, and the optimal approach will depend on the specific requirements of the application. The choice of the appropriate method should be based on a thorough evaluation of the method's suitability, accuracy, and computational efficiency.

In general, the stiffness of single pair of teeth can be described by equation (1)

$$c = \frac{w}{\delta}\ [N \cdot mm^{-1} \cdot \mu m^{-1}], \tag{1}$$

Where:

c…Stiffness of single pair of teeth in engagement [N mm^{-1} μm^{-1}],

w…Load along the face width in direction of the line of action [N mm^{-1}],

δ…Deformation of one pair of teeth [μm].

Similarly, the stiffness of double pairs of teeth can be defined by equation (1), with the load w being the sum of the load of the teeth of the first pair w1 and the load of the teeth of the second pair w2, which corresponds to the deformation δ.

2.1 Analytical Model in Terms of Strain Energy

The first analytical model for obtaining of the course of the mesh stiffness, designated as AM1 hereafter, is the strain energy method model reported in the publication of Zaigang Chen and Yimin Shao, [7] and Zhiguo Wan et al, [8]. This model is based directly on the theory of elasticity and considers each individual tooth as a cantilever beam located in a dedendum circle with a variable cross-section, where the force acts in the direction of the point of action.

The strain energy accumulated in the tooth is calculated individually for each tooth that comes into an engagement. The potential energies that contribute to the gear stiffness calculation include bending energy (U_b), shear energy (U_s), and axial compressive energy

(U_a). These energies can be determined using equations (2).

$$U_b = \frac{F^2}{2 \cdot K_b}\ [N \cdot mm],$$

$$U_s = \frac{F^2}{2 \cdot K_s}\ [N \cdot mm], \quad (2)$$

$$U_a = \frac{F^2}{2 \cdot K_a}\ [N \cdot mm],$$

Where:
K_b…Bending stiffness [N mm^{-1}],
K_s…Shear stiffness [N mm^{-1}],
K_a…Axial compressive stiffness [N mm^{-1}],
F…Force in direction of line of action [N].

The required contributing stiffnesses are given by equations (3) and the related scheme of loaded tooth is shown in Fig. 1.

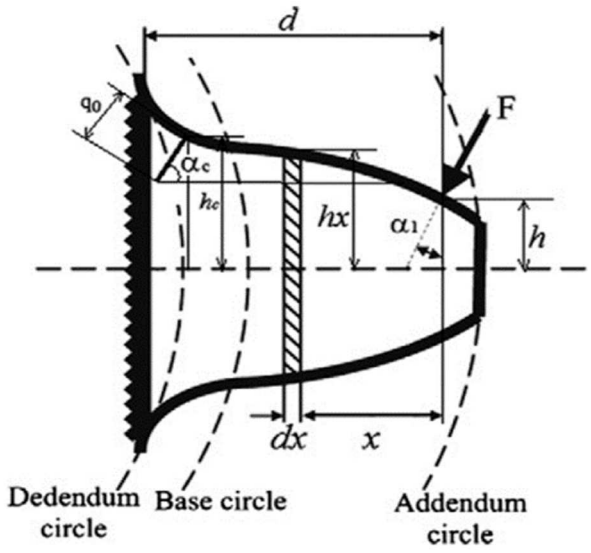

Fig. 1 *Geometrical parameters for mesh stiffness calculation [7]*

$$\frac{1}{K_b} = \int_0^d \frac{(x \cdot cos\ \alpha_1 - h \cdot sin\ \alpha_1)}{E \cdot I_x} dx\ [N^{-1} \cdot mm],$$

$$\frac{1}{K_s} = \int_0^d \frac{1.2 \cdot cos^2\ \alpha_1}{G \cdot A_x} dx\ [N^{-1} \cdot mm], \quad (3)$$

$$\frac{1}{K_a} = \int_0^d \frac{sin^2\ \alpha_1}{E \cdot A_x} dx\ [N^{-1} \cdot mm],$$

Where:
E…Young modulus [N mm^{-2}],
G…Shear modulus [N mm^{-2}],
A_x…Area of cross-section of tooth [mm^2],
I_x…Moment area of inertia [mm^4],
x…Distance between the section and acting point of the applied force (takes on values from 0 to d) [mm],
h…Half the thickness of the tooth at the acting point of the applied force [mm],
α_1…Angle of engagement [rad].

The contact stiffness is also reflected in the overall mesh stiffness of the gearing. This stiffness is referred to a Hertzian contact stiffness K_h, [7]. This stiffness is calculated by equation (4).

$$\frac{1}{K_h} = \frac{4 \cdot (1 - \nu^2)}{\pi \cdot E \cdot W}\ [N^{-1} \cdot mm], \quad (4)$$

Where:
ν…Poisson's ratio [-],
W…Face width [mm],
E…Young modulus [N mm^{-2}].

The final factor that influences the mesh stiffness of gearing is known as fillet-foundation stiffness K_f [6]. It re-presents the stiffness that accounts for the fillet radius and can be expressed by equations (5) and (6)

$$\frac{1}{K_f} = \frac{\delta_f}{F}\ [N^{-1} \cdot mm], \quad (5)$$

$$\delta_f = \frac{F \cdot \cos^2 \alpha_m}{W \cdot E} \cdot \left\{ L^* \cdot \left(\frac{u_f}{S_f}\right)^2 + M^* \cdot \left(\frac{u_f}{S_f}\right) + P^* \cdot (1 + Q^* \cdot \tan^2 \alpha_m) \right\}\ [mm], \quad (6)$$

Where:
δ_f…Deformation of tooth at its fillet radius [μm],
L^*, M^*, P^*, Q^*…Coefficients given by general polynomial function describing the geometry of fillet radius, [6], [-],
u_f…Distance of the center of force from the dedendum circle [mm],
S_f…Length of the dedendum arch of the tooth [mm],
α_m…Angle of engagement [rad],
W…Face width [mm],
E…Young modulus [N mm^{-2}].

The individual terms of equation (6) are shown in Fig. 2.

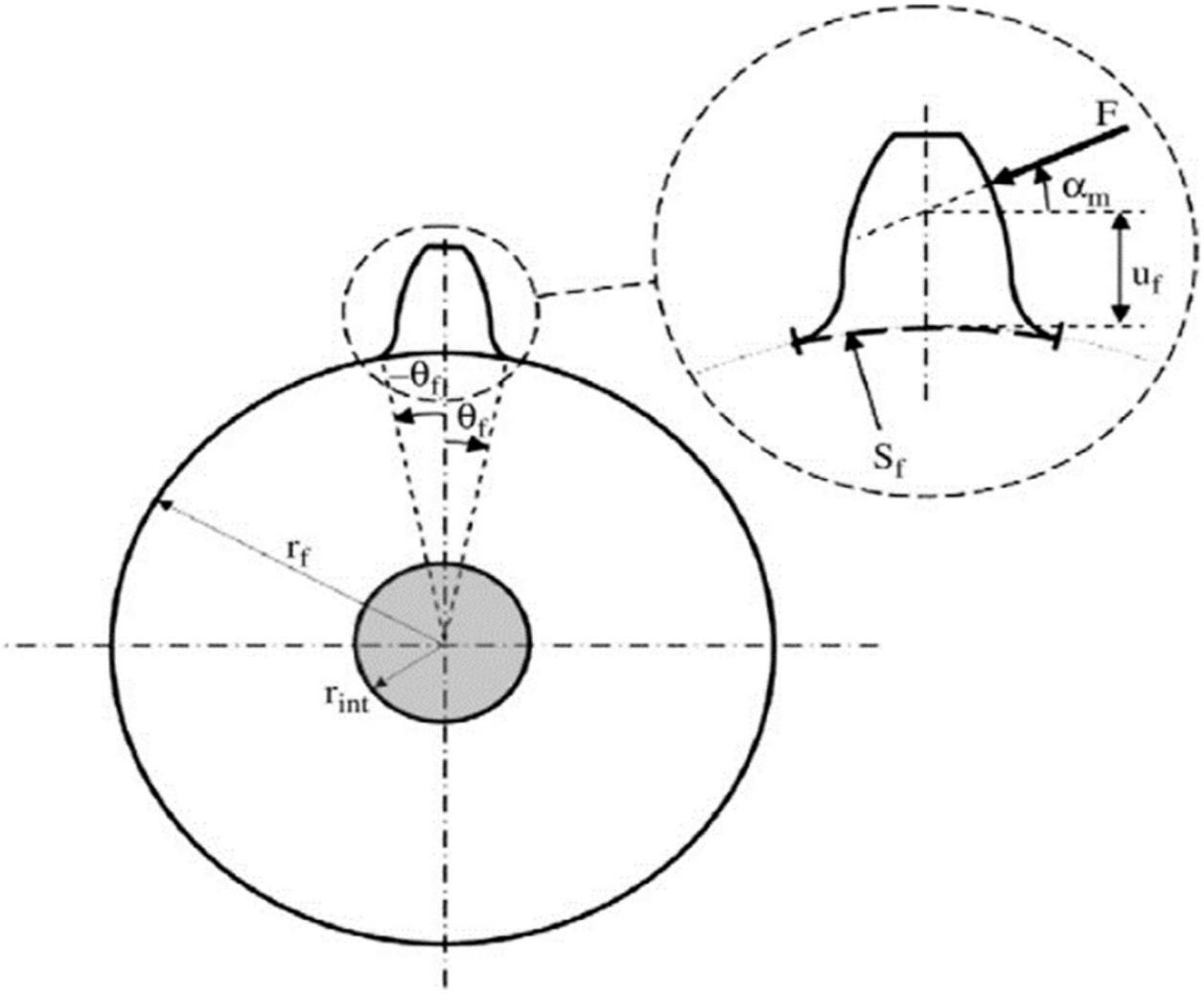

Fig. 2 *Geometrical parameters for fillet-foundation stiffness calculation* [7]

The total stiffness of single-pair K_1 and double-pairs K_2 of teeth in engagement is determined by equations (7) and (8).

$$K_1 = \frac{1}{\frac{1}{K_{b1}} + \frac{1}{K_{s1}} + \frac{1}{K_{a1}} + \frac{1}{K_{f1}}} + \frac{1}{\frac{1}{K_{b2}} + \frac{1}{K_{s2}} + \frac{1}{K_{a2}} + \frac{1}{K_{f2}} + \frac{1}{K_h}} [N \cdot mm^{-1} \cdot \mu m^{-1}], \tag{7}$$

$$K_2 = \sum_{i=1}^{2} \frac{1}{\frac{1}{K_{b1,i}} + \frac{1}{K_{s1,i}} + \frac{1}{K_{a1,i}} + \frac{1}{K_{f1,i}}} + \sum_{i=1}^{2} \frac{1}{\frac{1}{K_{b2,i}} + \frac{1}{K_{s2,i}} + \frac{1}{K_{a2,i}} + \frac{1}{K_{f2,i}} + \frac{1}{K_{h,i}}} [N \cdot mm^{-1} \cdot \mu m^{-1}], \tag{8}$$

2.2 KISSsoft Deformation Model of Mesh Stiffness

KISSsoft is a calculation software that facilitates the design, optimization, and verification of machine elements based on international standards. This software is also useful for carrying out calculations related to various types of gears, including generating the mesh stiffness course. It offers the capability to design gear geometry and per-form calculations related to the subject matter of this article. All calculation relationships mentioned below are obtained from the KISSsoft software manual [13].

The theory of mesh stiffness of gears used by the KISSsoft calculation software is also based on the deformati-on model of the teeth in engagement, similarly to the AM1 mentioned here. Tooth deformation can be split into three parts: gear body deformation, bending, and Hertzian flattening.

Gear body deformation δ_{RK} is given by equation (9) and the calculation scheme is in Fig. 3.

$$\delta_{RK} = \frac{F_{tbi}}{b} \cdot \cos^2 \alpha_{Fy} \cdot \frac{1-\nu^2}{E} \cdot \cdot \left\{ \frac{18}{\pi} \cdot \left(\frac{y_p}{s_{f20}} \right)^2 + \frac{2 \cdot (1-2\nu)}{1-\nu} \cdot \left(\frac{y_p}{s_{f20}} \right) + \frac{4.8}{\pi} \cdot \left(1 + \frac{(1-\nu)}{2.4} \cdot \tan^2 \alpha_{Fy} \right) \right\} [mm], \quad (9)$$

Where:
F_{tbi}…Force acting on the tooth [N],
b…Face width [mm],
α_{Fy}…Angle of engagement [rad],
E…Young modulus [N mm^{-2}],
ν…Poisson's ratio [-],
y_p…Distance of the center of force from the dedendum circle [mm],
s_{f20}…Length of the dedendum arch of the tooth [mm].

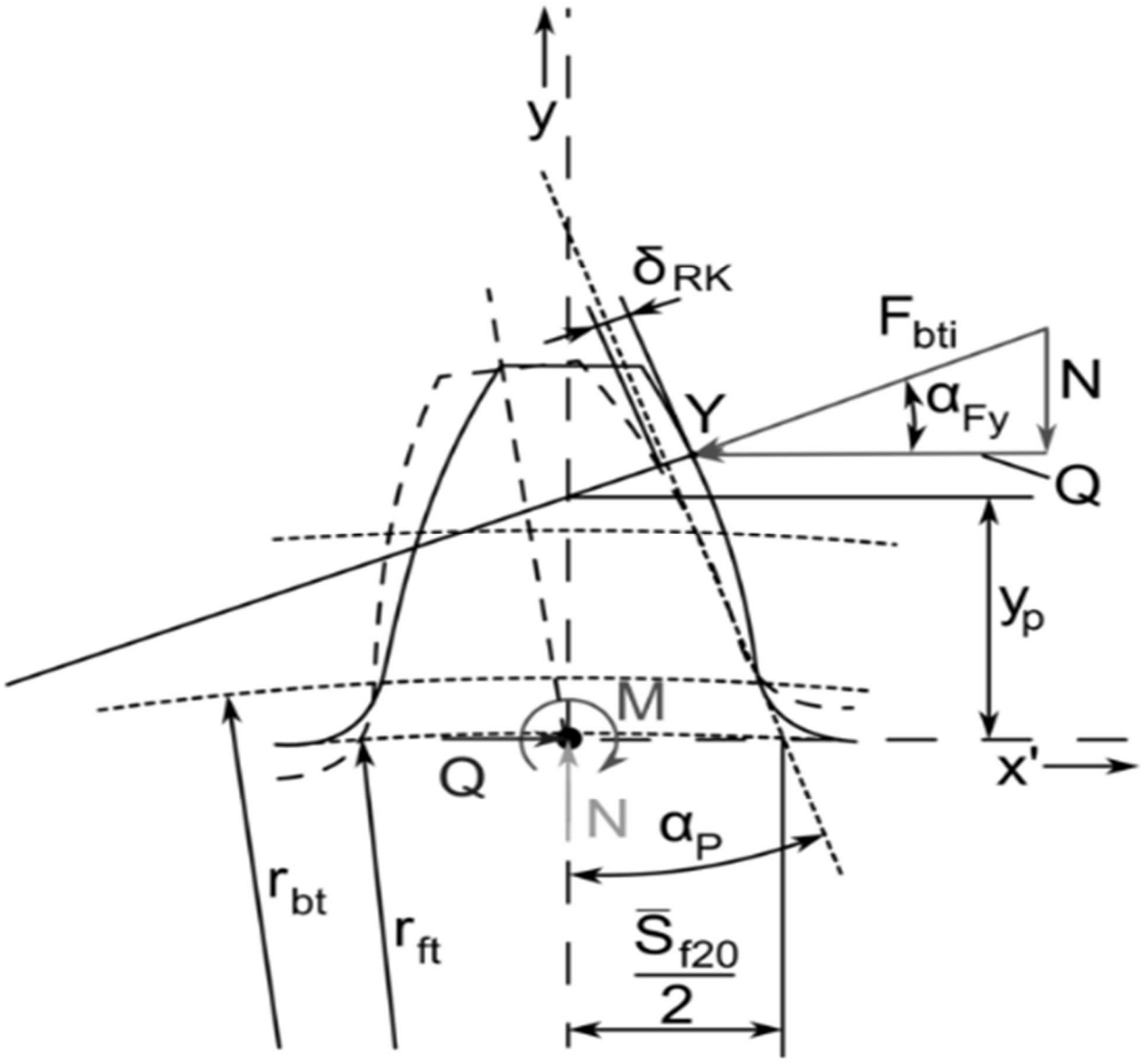

Fig. 3 *Gear body deformation scheme* [13]

It can be seen that the relationship given by equation (9) is almost identical to the relationship given by equati-on (8).

Bending deformation δ_B is given by equation (10) and the calculation scheme is in Fig. 4.

$$\delta_B = \frac{F_{tbi}}{b} \cdot \cos^2 \alpha_{Fy} \cdot \frac{1-\nu^2}{E} \cdot \left\{ 12 \cdot \int_0^{y_p} \frac{(y_p - y)^2}{(2x')^3} \, dy + \left(\frac{2.4}{1-\nu} + \tan^2 \alpha_{Fy} \right) \int_0^{y_p} \frac{dy}{2x'} \right\} [mm], \quad (10)$$

Where:
F_{tbi}…Force acting on the tooth [N],
b…Face width [mm],
α_{Fy}…Angle of engagement [rad],
E…Young modulus [N mm^{-2}],
ν…Poisson's ratio [-],
y_p…Distance of the center of force from the dedendum circle [mm],
y…Total tooth height [mm],
x'…Variable tooth thickness [mm].

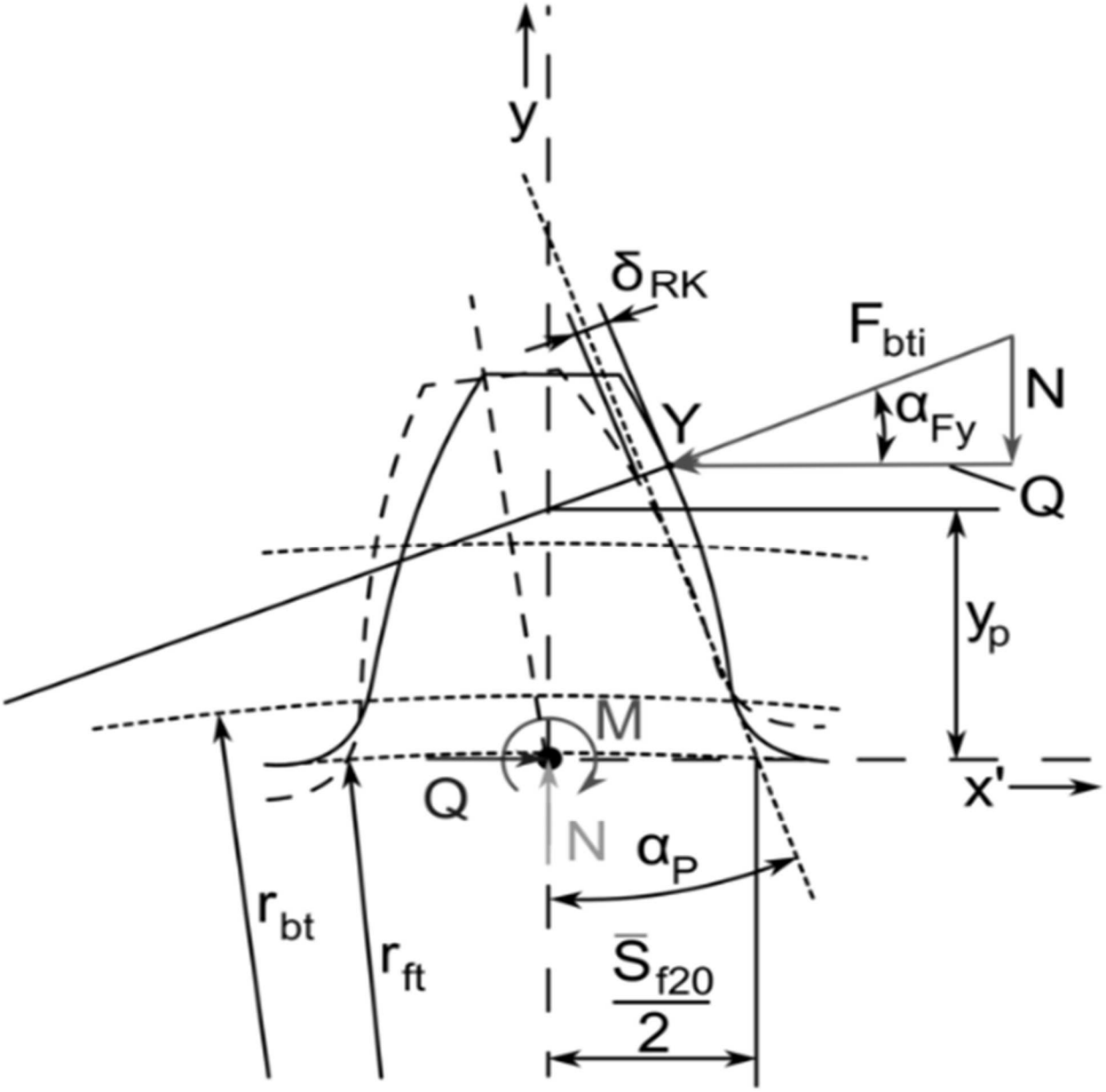

Fig. 4 *Bending deformation scheme* [13]

Hertzian flattening $\delta_{H1,2}$ is described by equation (11) and the calculation scheme is in Fig. 5.

$$\delta_{H1,2} = \frac{F_{tbi}}{\pi b_g} \cdot \left\{ \left| \frac{1-\nu_1{}^2}{E_1} \ln\left(\frac{b_H{}^2}{4t_1{}^2}\right) + \frac{\nu_1(1-\nu_1)}{E_1} \right| + \left| \frac{1-\nu_2{}^2}{E_2} \ln\left(\frac{b_H{}^2}{4t_2{}^2}\right) + \frac{\nu_2(1-\nu_2)}{E_2} \right| \right\} [mm], \quad (11)$$

Where:
F_{tbi}…Force acting on the tooth [N],
bg…Contact face width [mm],
bh…Size of the contact area [mm],
$E_{1,2}$…Young modulus of gear tooth 1 and gear tooth 2[N mm-2],
$\nu_{1,2}$…Poisson's ratio of gear tooth 1 and gear tooth 2 [-],
$t_{1,2}$…Radius of curvature of the side curve of the tooth at the point of contact of gear tooth 1 and gear tooth 2 [mm].

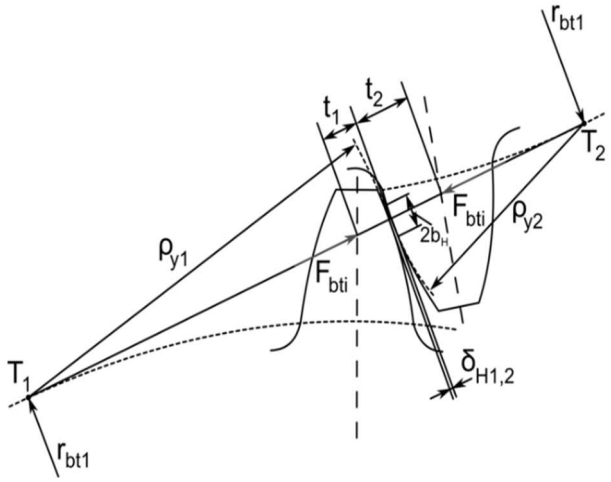

Fig. 5 *Hertzian flattening scheme* [13]

The total deformation δ has the effect that the contact point is displaced along the path of contact and the theo-retical length of path of contact is elongated, in comparison to the actual length of path of contact.

The spring equation (12) can be applied to calculate the components of the single contact stiffness *C* from the individual deformation components and the normal force.

$$F = \delta \cdot C\ [N], \tag{12}$$

Where:

F…Normal force [μm],

δ…Generalized deformation of tooth of gear [mm],

C…Generalized single contact stiffness [mm].

The following equation (13) applies for the tooth pair spring stiffness in a meshing gear pair.

$$\frac{1}{C} = \frac{1}{C_{B1}} + \frac{1}{C_{R1}} + \frac{1}{C_{B2}} + \frac{1}{C_{R2}} + \frac{1}{C_{H1,2}}\ [N \cdot mm^{-1}], \tag{13}$$

Where:

C_{B1}…Bending stiffness of the first pair of teeth [N mm^{-1}].

C_{B2}…Bending stiffness of the second pair of teeth [N mm^{-1}].

C_{R1}…Gear body stiffness of the first pair of teeth [N mm^{-1}].

C_{R2}…Gear body stiffness of the second pair of teeth [N mm^{-1}].

$C_{H1,2}$…Hertzian contact stiffness of teeth [N mm^{-1}].

2.3 FEM Model

Several published studies have validated the analytically calculated mesh stiffness of gear system using Finite Element Method (FEM) simulations. The FEM approach for determining mesh stiffness is commonly documented in these works, [11, 14-16]. Researchers typically resort to this method when they lack empirical data obtained from experimental mesh stiffness measurements. Nevertheless, it is important to verify the FEM results, as this approach is highly reliant on the accuracy of the model definition.

In this case, boundary conditions were established for the calculation process, taking into account the place-ment of the pinion and gear. The gear model was designed as planar since it is a spur gear with straight teeth, with only rotation around its own axis of rotation allowed. The boundary conditions also included predefined rotations of the pinion and gear, which were used to define tooth backlash and enable common rotation.

The boundary conditions and the torque load of the wheel (53.75 Nm) were gradually applied over three com-putational steps. A very fine mesh of the pinion (111,968 elements) and gear (83,952 elements) was created using CPS8R-type elements, which are quadrangular elements suitable for planar stress analysis. The boundary conditions, encompassing rotational parameters and load torque, are illustrated in Fig. 6. The figure also displays the configuration of an exceedingly refined mesh applied to the gear teeth. For this calculation, the Young's modulus equ-al to 3200 MPa was chosen, which corresponds to plexiglas. The reason why plexiglass was chosen is described in section 3.2.

Using FEM analysis, the deformation rotation of the pinion and gear was determined, and this was converted into the stiffness of compression springs inserted between perfectly rigid teeth. The stiffness of the gears was thus obtained in [N mm^{-1} μm^{-1}] units.

The resulting mesh stiffness kc obtained from the FEM calculation was determined from the equation (14).

$$k_c = \frac{k_p \cdot k_g}{k_p + k_g}\ [N \cdot mm^{-1} \cdot \mu m^{-1}], \tag{14}$$

Where:

k_p…Stiffness of the pinion teeth [N mm^{-1} μm^{-1}],

k_g…Stiffness of the gear teeth [N mm^{-1} μm^{-1}].

The stiffnesses k_p and k_g depend on the load and the deformation rotation of pinion δ_p and gear δ_g in [μm] unit, which are the result of the FEM analysis.

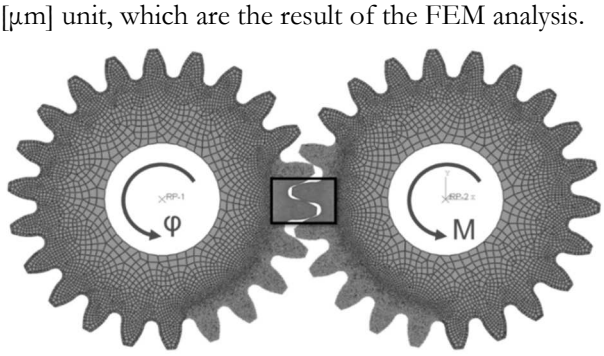

Fig. 6 *Boundary Conditions of FEM Calculation*

3 Experimental Determination of Mesh Stiffness

In the preceding chapters, the most commonly used analytical-simulation models for describing gearing stiffness were briefly discussed. This chapter is devoted to the primary contribution of this work, which focuses on the experimental determination of mesh stiffness of gearing. The following paragraphs provide a description of the custom testing equipment and the principle of its use for obtaining real stiffness courses. Additionally, this text covers the selection of initial test specimens and the instrumentation of the entire apparatus.

3.1 Description and Function of Measurement Rig

To obtain a mesh stiffness course of a gearing system, it is necessary to measure the angular deformation of te-eth of gearing during an engagement. However, to ensure the measured deformation is not affected by the deformations of other components of the test rig in the experimental setup, the stiffness of the entire structure must be significantly higher than that of the examined gearing. Accordingly, the design of the test device must fulfill this requirement.

Measuring mesh stiffness is a straightforward task in principle. The gear is loaded with torque, which in this ca-se is achieved using a suspended weight (Force G) on the load lever that is part of the input gear (pinion). The out-put gear is then braked using a pair of screws with attachments that exert force on its sides. The friction effect between the attachments and the gear disc generates a force (F_{BR}), which stops the output gear. The principle described above is illustrated in Fig. 7.

The experimental setup was designed to be modular and enable efficient and cost-effective measurement of gearing deformations to obtain a realistic mesh stiffness course. Modularity is ensured primarily through the spe-cially designed geometry of the gear segments used as specimens (as described in section 3.2). Fig. 8 shows the resulting model of the experimental device construction.

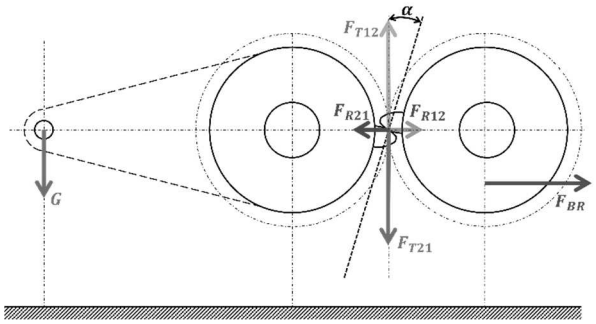

Fig. 7 *3D The Principle of Function of Measurement Rig*

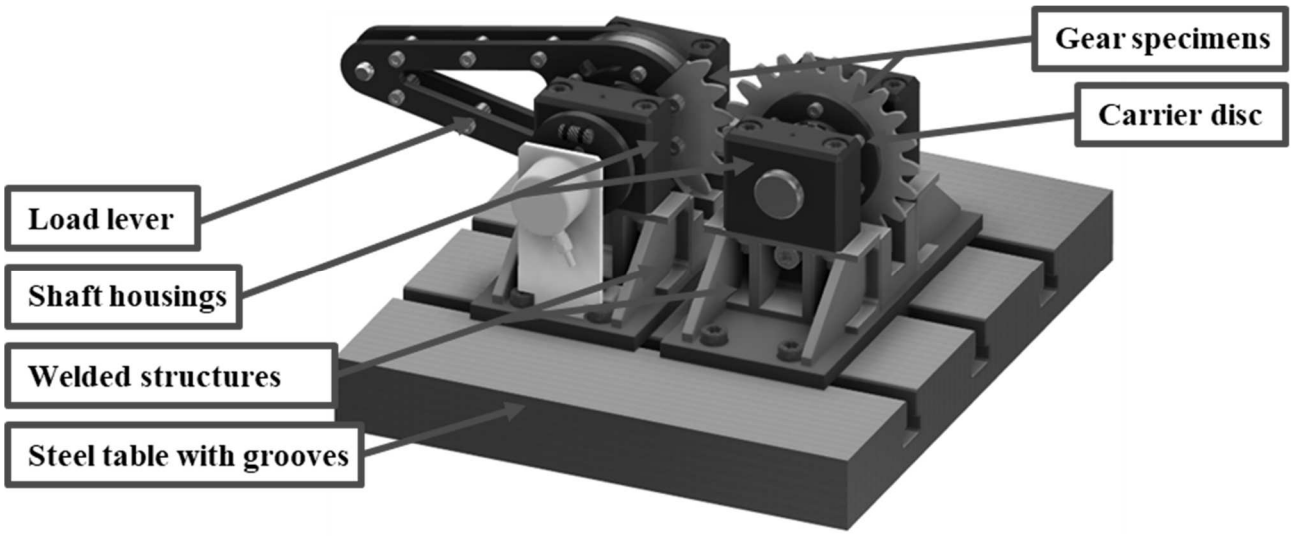

Fig. 8 *3D model of the experimental test rig*

The experimental rig consists of two welded structures mounted on a steel table with grooves. The shaft housings are fixed to the weldments using screws, and they are designed as plain bearings to minimize the tilting of the shafts in the supports. These welded structures, along with the shaft housings, provide the foundation for mounting the shafts (axles), which are equipped with carriers for attaching gear samples or load lever. The carrier discs are fixed on the shafts using clamping sleeves. This method of attaching the hub to the shaft was chosen to ensure the maximum modularity of the entire experimental setup. The load lever is connected to the carrier disk in a way that ensures that the gear specimen is loaded in its midplane, preventing any uneven distribution of the load across its width. The diameter of the gear specimen is centered on the respective diameter of the carrier disk,

while its side surface is supported by an insert that is part of the load lever. The gear samples are attached to the driving disk using screws that are intended to ensure the position of the segment in the axial direction of the shaft, rather than to secure the sample by force. The clamping screws should not perform a force function, as this would artifi-cially reinforce the segment and result in an unrealistic load on the gearing. The output gear is attached to a carrier disc on the output shaft, similar to what was previously described for the input gear variant. Unlike the input gear, the output gear pattern is not formed as a segment, but rather as a disk that combines multiple gear geometries. This disk is braked by screws that generate frictional force.

The entire apparatus has been meticulously designed to prevent any twisting of the shafts, which could otherwise affect the deformation of the gear teeth. At the end of the freely rotating input shaft with the load lever, the angular rotation can be read, which in this case is the deformation rotation caused by the engagement of the gear teeth.

3.2 Test specimens

The mesh stiffness of the gearing was determined based on the gear specimens. In the case of the input gear (pinion), the gear is represented by segments of the entire gear, as shown in Fig. 9a. The output gear combines two toothed profiles, as depicted in Fig. 9b.

This methodology was designed to minimize the cost of producing samples and to make the process of determi-ning the mesh stiffness of the gearing more accessible and easily modifiable. The purpose of constructing samples in this way is solely to achieve these goals.

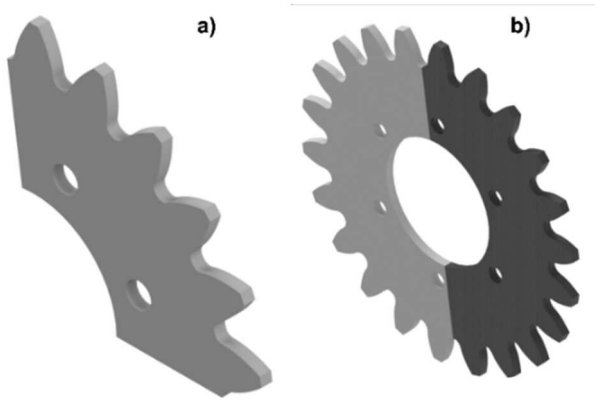

Fig. 9 *The geometry of used gearing samples, a) input gear segmnet (pinion), b) output combined gear*

The segments of input gears and combined output gears used as samples are characterized by specific properties, such as their width (i.e., gear width) and material. In this study, plexiglass samples with a width of 5 mm were utilized, which was chosen based on the ability to accurately measure deformations. It is essential that the stiffness is measurable under laboratory conditions and that the measured data is not significantly affected by measurement uncertainties. The material used for these samples was selected because it was the first time testing on this device, and it was necessary to visually inspect the contact points of the sides of the gear teeth. Moreover, these samples can be used for future verification by utilizing photoelasticity.

The basic parameters of the selected gears (ISO 53 standard) for this paper are as follows:

- Normal module m_n=8mm,
- Gear width b=5mm,
- Pressure angle α=20°,
- Helix angle β=0°,
- Number of teeth pinion z_1=22 and gear z_2=22,
- Profile shift coefficient of gear x_2=0,
- Profile shift coefficient of pinion x_1=0,
- Center distance a_w=176 mm.

From the outset, the design for producing samples was intended to incorporate alternative production methods as opposed to conventional gear production methods, primarily due to economic considerations. Based on the proposed tooth width of 5 mm, laser machining was selected as the production method of choice.

3.3 Instrumentation

The experimental device is primarily designed to measure the angular deformation of the teeth in engagement from the free end of the input shaft, to determine the stiffness of the gearing. This is achieved through the use of an incremental sensor DFS 60 Inox, which is specifically designed for sensing angular rotation or revolutions. The sensor is connected to the free end of the shaft using a mounted flange and coupling. The sensor utilized in the experimental rig is capable of detecting rotation in the order of thousands of angular degrees, making it suitable for this application. The deformation rotation of the gearing system typically reaches values in the order of lower tenths to higher hundredths of angular degrees, rendering the sensor suitable for measuring the deformation rotation. In addition, the rotation sensor enables analysis of the global angular position of the input gear in engagement. Consequently, the deformation rotation can be graphically displayed directly, dependent on the overall angular position of the gear. The distance between the input segment gear (pinion) and the output gear is determined by the center-to-center distance of shafts, which is measured using a TMLS-01S-02 magnetic linear encoder with a mea-surement accuracy of +/-

10μm. This method ensures a high level of precision in the measurement of the distance between the two gears.

4 Results

In this chapter, are presented the results of mesh stiffness obtained through analytical-simulation methods. Ad-ditionally, the preliminary results of experimental test measurements of gear stiffness are provided.

In order to clearly present the results of this study, it is imperative to specify the magnitude of the torque exer-ted on the gear train in the context of analytical calculations and experimental measurements. The applied torque for loading the gear was 53.75 Nm. This particular torque value was selected to ensure the preservation of linear material behavior and to prevent any permanent deformations or fractures of the plexiglass gears. Throughout the experiment, the torque was generated by employing multiple weights, which, in conjunction with the load lever's own weight, collectively contributed to the aforementioned torque exerted on the lever's arm.

4.1 Results Obtained by Analytical-simulations Methods

In relation to the designed gearing (refer to section 3.2), the variation of gearing stiffness was assessed using Analytic simulation models AM1, KISSsoft, and FEM. These models were previously detailed in Chapter 2. The selection of multiple gear stiffness models was deliberate, aiming to facilitate a clear and unequivocal interpretati-on of the experimental outcomes. This section outlines the fundamental distinctions between the employed analy-tical simulation models.

During the process of gear engagement, one or two pairs of teeth undergo alternating engagement. This observa-tion is visually evident in Fig. 10 (Single-Pair and Double-Pair Mesh Stiffness), where the obtained results of the mesh stiffness courses, generated through analytical-simulation methods, are presented. When two pairs of teeth are simultaneously engaged, the stiffness of the tooth engagement – mesh stiffness is notably higher compared to the scenario where only one pair of teeth is engaged.

A concise summary of the findings is presented in Tab. 1. Tab. 1 provides the average values for the various states of engagement, specifically the mesh stiffness of individual gear pairs (Single-Pair Mesh Stiffness) and the mesh stiffness of two gear pairs (Double-Pair Mesh Stiffness), for the sake of clarity. When comparing these valu-es, the Finite Element Method (FEM) is considered the benchmark, as it closely approximates the actual expressi-on of mesh stiffness. Therefore, the analytical methods AM1 and KISSsoft are compared to the FEM method, rather than being compared to each other. Tab. 1 also presents the percentage differences between the average values of Single-Pair Mesh Stiffness and Double-Pair Mesh Stiffness in relation to the FEM method.

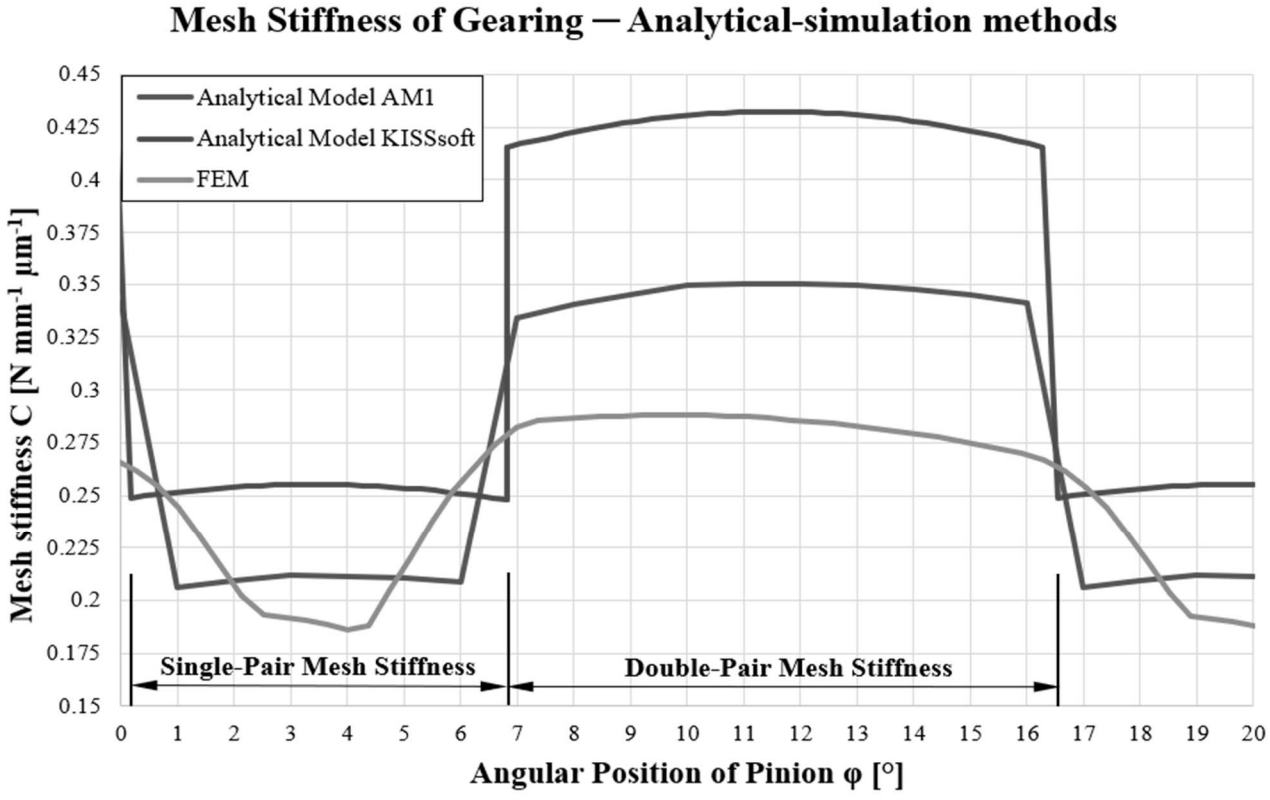

Fig. 10 *Results of Analytical-Simulation Methods*

Tab. 1 *Mean Values of Mesh Stiffness [N mm-1 μm-1] – Comparisson of Analytical-Simulation Methods*

Single-Pair Mesh Stiffness					
	AM1	KISSsoft	FEM	Δ AM1 – FEM [%]	Δ KISSsoft – FEM [%]
Tested Gearing	0.209	0.252	0.189	10.58	33.33
Double-Pair Mesh Stiffness					
	AM1	KISSsoft	FEM	Δ AM1 – FEM [%]	Δ KISSsoft – FEM [%]
Tested Gearing	0.342	0.424	0.278	23.02	52.52

Based on the graph depicted in Fig. 10 and the information provided in Tab. 1, it is evident that significant disparities exist among the individual theoretical models and approaches. Consequently, it is strongly recommended to undertake experimental verification of the determined mesh stiffness. This is necessary as it is not possible to definitively determine which method aligns closest to reality solely based on the calculation models.

The percentage difference between the AM1 and FEM methods for single-pair mesh stiffness is 10.58 %, while for double-pair mesh stiffness, it amounts to 33.33 %.

In terms of the comparison between the KISSsoft mathematical model and the FEM calculation, the variations are notably distinct when expressed in percentages. Specifically, there is a 23.02 % difference in the realm of sin-glene-pair mesh stiffness and a 52.52 % difference in the realm of double-pair mesh stiffness.

The primary disparities observed in the mesh stiffness courses obtained through the AM1 method and the KISSsoft model arise from variations between the two models (Fig. 10). Despite their inherent similarities, the mo-deling approaches for Fillet-foundation Stiffness (AM1) and Gear Body Stiffness (KISSsoft) differ. While the KISSsoft model essentially employs the same underlying model (equation (9)) as the AM1 method, there are more precise specifications of the constants describing the geometry of the tooth root region in equation (6) within the AM1 method. Moreover, the geometry of the tooth heel is further refined using polynomials denoted by the sym-bols L*, M*, P*, Q* in the AM1 method. These distinctions significantly impact the resulting mesh stiffness courses.

Another distinction lies in the employment of the contact stiffness model. The KISSsoft method incorporates a sophisticated contact stiffness model, as seen in equation (11), while the AM1 model utilizes a simplified model depicted in equation (4). These differences contribute to the varying mesh stiffness profiles displayed in Fig. 10.

The individual courses of the calculated mesh stiffnesses (Fig. 10) also exhibit variations compared to the FEM courses of the mesh stiffness and the experimentally determined mesh stiffness. The interpretation of these dispa-rities is provided in the subsequent section, namely Section 4.2.

4.2 Results Obtained by Experimental Measurement

In Section 4.1, the courses of mesh stiffness of gearing obtained through analytical-simulation methods were found to be challenging to interpret. This difficulty arises due to the significant percentage differences observed among the resulting courses of mesh stiffness, which span magnitudes of tens of percent. Consequently, it remains uncertain which variant of the analytical simulation calculation can be confidently deemed as closely approxima-ting reality.

Hence, the objective was to initiate experimental measurements of mesh stiffness in a test configuration using the aforementioned gear specimens. This endeavor aimed to ascertain whether analytical-simulation models of mesh stiffness, while considering certain deviations from reality, can be employed, or if it is imperative to procure experimental data for the dynamic analysis of the gear transmission that most accurately depicts the actual beha-vior of the engaged gear teeth.

Fig. 11 illustrates the courses of mesh stiffness of tested gearing obtained through analytical-simulation met-hods, similar to those presented in the previous chapter (Fig. 10). The purpose of including these courses is to faci-litate a comparative and evaluative analysis of the experimental measurement, which ultimately yield the realistic mesh stiffness. Fig. 11 presents the data obtained through Experimental Measurement, depicted in black.

The results of the comparison between analytical-simulation methods and the experimental approach are con-cisely presented in Tab. 2. The table provides an assessment of mean mesh stiffness values in both Single-Pair Mesh Stiffness and Double-Pair Mesh Stiffness states. To facilitate a comprehensive comparison of all the met-hods employed, the experimental measurement was selected as the reference, representing the most accurate eva-luation of the actual manifestation of gear stiffness in real-world conditions. Consequently, the AM1, KISSsoft, and FEM methods were compared against the experimental data. Tab. 2 summarizes this comparison by presenting the percentage differences between the aforementioned methods.

Tab. 2 *Mean Values of Mesh Stiffness [N mm⁻¹ μm⁻¹] – Comparisson of Experimental Measurement and Analytical-Simulation Methods*

Single-Pair Mesh Stiffness							
	AM1	**KISSsoft**	**FEM**	**EXP**	**Δ AM1 – EXP [%]**	**Δ KISSsoft – EXP [%]**	**Δ FEM – EXP [%]**
Tested Gearing	0.209	0.252	0.189	0.185	12.97	36.22	2.16
Double-Pair Mesh Stiffness							
	AM1	**KISSsoft**	**FEM**	**EXP**	**Δ AM1 – EXP [%]**	**Δ KISSsoft – EXP [%]**	**Δ FEM – EXP [%]**
Tested Gearing	0.342	0.424	0.278	0.255	34.11	66.27	9.02

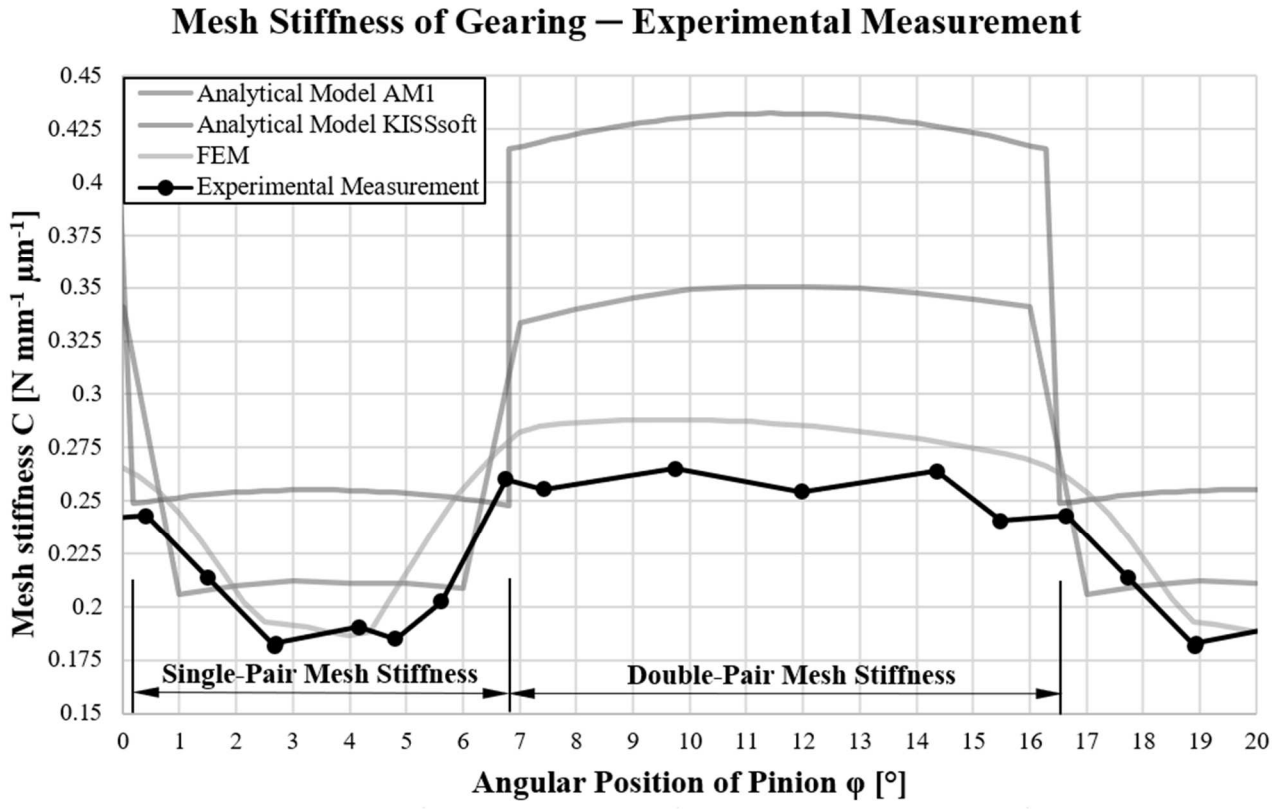

Fig. 11 *Comparison of Analytical-Simulation Methods and Experimental Measurement*

When examining the comparison between the mesh stiffness courses of gearing in Fig. 11 and the correspon-ding mean values of single-pair and double-pair mesh stiffness as presented in Tab. 2, it becomes evident that the simulation model implemented through Finite Element Method (FEM) analysis exhibits the closest resemblance to the experimentally measured data (referred to as EXP in Tab. 2). In summary, the percentage differences between the different methods are displayed here.

The percentage difference between AM1 and EXP method for single-pair mesh stiffness is 12.97 %, while for double-pair mesh stiffness it is 34.11 %.

Regarding the comparison between the KISSsoft mathematical model and the experimental measurement EXP, the percentage deviations are significant. Specifically, there is a 36.22 % difference in the area of single-pair mesh stiffness and a 66.27 % difference in the area of double-pair mesh stiffness.

Substantial disparities in the mesh stiffness of gears are observed when comparing the stiffness courses obta-ined through simulation calculations using the Finite Element Method (FEM) and experimental measurements (EXP). In this particular scenario, the deviation in the single-pair mesh stiffness is calculated to be 2.16%, while the percentage deviation in the double-pair mesh stiffness amounts to 9.02%.

At the end of section 4.1, a note was mentioned about the difference in the shapes of the obtained curves of courses the mesh stiffness of gearing (see Fig. 10 and Fig. 11), so this note is followed up here.

Within the realm of analytical models, specifically

the AM1 and KISSsoft models, a conspicuous and sharp al-ternation in the engagement phases is observed, namely between the single-pair and double-pair engagements. Naturally, alternations in the type of engagement are also manifested in the resultant profiles of mesh stiffness. On the contrary, the simulation model, specifically the Finite Element Method (FEM) model, exhibits a resemblance in shape to the stiffness profile obtained through experimental measurements. The transition between single-pair stiffness and double-pair stiffness is less abrupt and sharp compared to the AM1 and KISSsoft approaches.

The discernible dissimilarity in the profiles of the gear stiffness curves can be attributed to a definitive un-derstanding of the underlying calculation mechanism. Analytical models of mesh stiffness, such as AM1 and KISS-soft, operate under the assumption of ideal, undeformed gear geometry. All dimensional parameters pertaining to the gears, as inputted into the calculation models, adhere to the standard gear geometry specified in ISO 53 stan-dard. Consequently, these models do not account for the deformed state of the gear teeth. As a result, the transition between single-pair and double-pair mesh stiffness manifests as sudden and sharp. In accordance with the concep-tualization of the idealized model depicting a rolling spur gear with straight teeth, the occurrence of single-pair engagement and double-pair engagement is distinctly delineated.

Conversely, there exists a mesh stiffness model derived through Finite Element Method (FEM) calculations, as well as a mesh stiffness course derived from experimental measurements. These two approaches adopt entirely distinct perspectives on the behavior of the engaged gear teeth, despite both methods are different. The FEM model remains classified within the realm of analytical-simulation methods, whereas the measured data are obtained through actual experiments. To comprehend the distinct shapes of the mesh stiffness curves, it is essential to acknowledge the influence of loading on the gears through the application of torque. This loading induces defor-mation not only in the engaged teeth themselves but also in the overall gear teeth and gear disc. Consequently, a scenario arises where, during the intended measurement of stiffness for a single pair of teeth according to the AM1 and KISSsoft models, the deformation of the entire gear causes the engagement of a second pair of teeth that idea-lly should not be in the engagement. During the experimental measurement of mesh stiffness and the determination of mesh stiffness through FEM analysis, a situation arises where a single pair of teeth engages for a considerably shorter duration. Specifically, the duration of single-pair meshing is approximately 66.4 % shorter compared to the theoretical models of AM1 and KISSsoft. The aforementioned observation, pertaining to the paragraph discussed above, is visually depicted in Fig. 12.

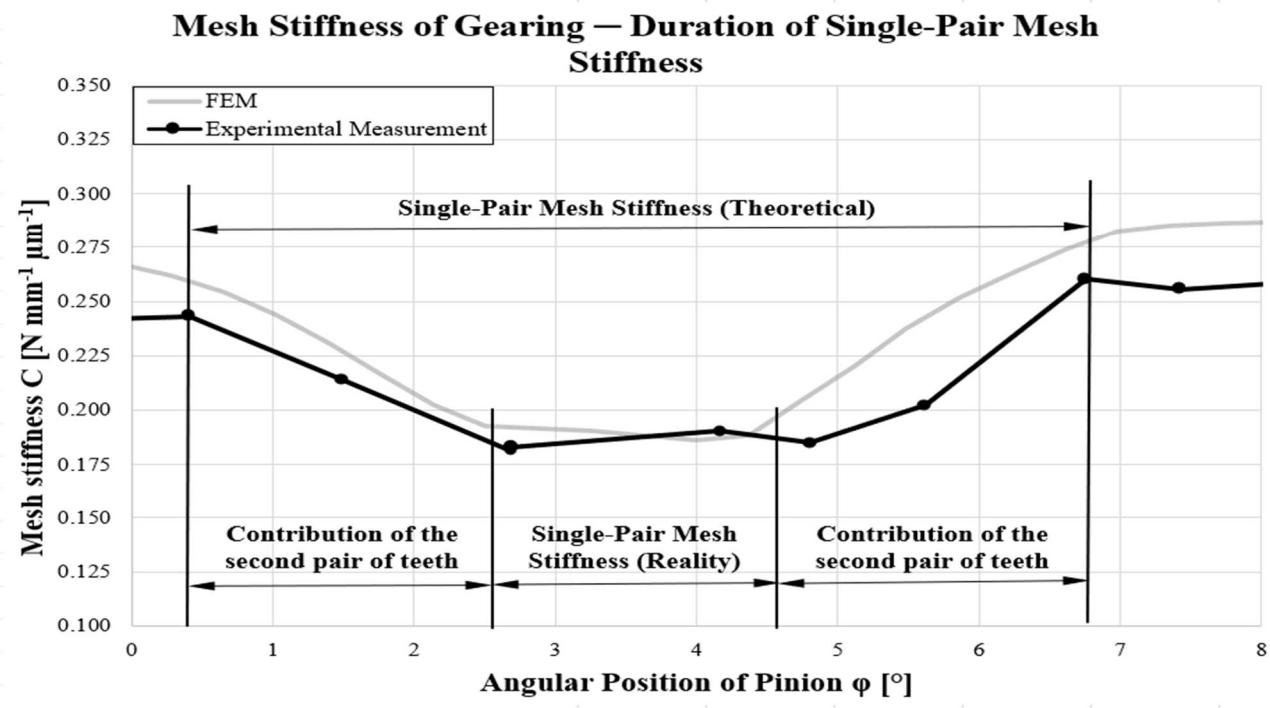

Fig. 12 *Comparison of theoretical and real single-pair mesh stiffness*

5 Conclusions

The objective of this article was to conduct an experimental verification of analytical-simulation models of mesh stiffness of gears and provide insights into the employed computational models. The article discussed the theoretical models suitable for evaluating mesh stiffness, including the deformation energy-

based calculation vari-ant (AM1), which offers advantages in accurately describing the theoretical geometry of gear teeth and its adjusta-bility. However, the adjustability of this model also presents potential drawbacks. It allows for the construction of a complete mesh stiffness model from partial stiffness models that participate in individual stiffness gear teeth, but these models may involve simplifications and may not necessarily be highly accurate.

An example of such simplification is the representation of contact stiffness in gearing in model AM1. The ove-rall accuracy of the gear stiffness model relies on the accuracy of the precise sub-models of stiffness incorporated within it. On the other hand, the KISSsoft computational model, which is directly integrated into the commercially available KISSsoft software, closely resembles the AM1 model. However, since it is a pre-implemented solver within the software, it cannot be further modified. This model exhibits highly accurate representation of contact stiffness but comparatively poorer description of the stiffness of the tooth root region, as mentioned in section 4.1.

The comprehensive assessment indicates that the AM1 model exhibits greater proximity to reality compared to the KISSsoft model. This finding strongly suggests the potential for further refinement of the AM1 model based on experimental measurements, thereby enabling the development of a highly precise tool for determining mesh stiffness that aligns with real-world conditions.

Upon evaluation, the utilization of FEM calculation for determining mesh stiffness has proven to be a reliable approach, exhibiting remarkably similar results to those obtained through experimental measurements. The devia-tion in single-pair stiffness amounted to 2.16 %, while the deviation in double-pair stiffness reached 9.02 %. These deviations can be considered highly accurate when compared to the significant deviations observed in the analyti-cal models, which differed by tens of percent. Notably, the KISSsoft model exhibited the poorest description of stiffness, with deviations of up to 66.27 % from the experimental measurements.

The presented experimental approach delivers a definitive message regarding the assessment of analytical-simulation methods employed in determining mesh stiffness. When aiming for the utmost accuracy in determining gear stiffness for dynamic calculations, the utilization of an experimental approach or the calculation of mesh stiffness through FEM analysis becomes imperative.

FEM analysis is known to be relatively time-consuming and financially demanding, particularly with regard to the costs associated with purchasing the license. Conversely, experimental verification offers an effective means of exploring the possibilities for accurately determining the mesh stiffness course of a given gear.

From the perspective of capturing the actual mesh stiffness course, it is crucial to account for the deformation of gear teeth (as discussed in section 4.2), a consideration that analytical approaches fail to accommodate.

Acknowledgement

This contribution was funded by Czech Technical University in Prague grant number SGS23/107/OHK2/2T/12.

References

[1] ZHANG, L., XU, W., ZHI, Y., HOU, N., LI, H., WANG, C., et al.. Optimization of Tooth Profile Modification and Backlash Analysis of Multi-tooth Mesh Cycloid Transmission. *Manufacturing Technology*. 2024;24(1): 154-163. doi: 10.21062/mft.2024.012

[2] ZHANG, L., ZHENG, T., LI, T., WANG, J., WANG, C., JIANG, Y., et al.. Precision Forming Process Analysis and Forming Process Simulation of Integrated Structural Gear for New Energy Vehicles. *Manufacturing Technology*. 2023;23(6):958-966. doi: 10.21062/mft.2023.102

[3] ČERNOHLÁVEK, V., SVOBODA, M., ŠTĚRBA, J., CHALUPA, M., SAPIETA, M.: Analytical and experimental solution of vibrations of a system of bound bodies, In: *Manufacturing Technology*, Vol. 20, No 6 (2020), pp. 699-707, ISSN: 1213-2489, DOI: 10.21062/mft.2020.116

[4] ŠMERINGAIOVÁ, A. Elimination of resonant phenomena adverse effect in the process of experimental operation of gears. *Manufacturing Technology*. 2021;21(6):842-848. doi: 10.21062/mft.2021.087

[5] VAŠINA, M., HRUŽÍK, L., BUREČEK, A. Study of Factors Affecting Vibration Damping Properties of Multi-layer Composite Structures. *Manufacturing Technology*. 2020;20(1):104-109. doi: 10.21062/mft.2020.019

[6] SAINSOT, P., VELEX, P., DUVERGER, O. (2007). Contribution of Gear Body to Tooth Deflections—A New Bidimensional Analytical Formula. *Journal of Mechanical Design*, volume 126, issue 4, Springer, pp. 748 – 752. Available at: https://doi.org/10.1115/1.1758252

[7] CHEN, Z., SHAO, Y. (2011). Dynamic simulation of spur gear with tooth root crack propagating alog tooth width and crack depth. *Engi-*

neering Failure Analysis, volume 18, issue 8, Elsevier, pp. 2149 – 2164. Available at: http://www.sciencedirect.com/science/article/pii/S1350630711001816

[8] WAN, Z., CAO, H., ZI, Y., HE, W., HE, Z. (2014). An improved time-varying mesh stiffness algorithm and dynamic modeling of gear-rotor system with tooth root crack. *Engineering Failure Analysis*, volume 42, Elsevier, pp. 157 – 177. Available at: https://www.sciencedirect.com/science/article/abs/pii/S1350630714001125

[9] SAXENA, A., CHOUKSEY, M., PAREY, A. (2017). Effect of mesh stiffness of healthy and cracked gear tooth on modal and frequency response characteristics of geared rotor systém. *Mechanism and Machine Theory*, issue 107, Elsevier, pp. 261 – 273. Available at: https://www.sciencedirect.com/science/article/abs/pii/S0094114X16303615

[10] LI, Z., ZHU, C., LIU, H., GU, Z. (2020). Mesh stiffness and nonlinear dynamic response of a spur gear pair considering tribo-dynamic effect. *Mechanism and Machine Theory*, issue 153, Elsevier. Available at: https://www.sciencedirect.com/science/article/abs/pii/S0094114X2030210X

[11] FLEK, J., DUB, M., KOLÁŘ, J., LOPOT, F., PETR, K. (2021). Determination of Mesh Stiffness of Gear – Analytical Approach vs. FEM Analysis. *Applied Sciences*, volume 11, issue 11, MDPI. Available at: https://www.mdpi.com/2076-3417/11/11/4960

[12] KONG, Y., JIANG, H., DONG, N., SHANG, J., YU, P., LI, J., YU, M. (2023) Analysis of Time-Varying Mesh Stiffness and Dynamic Response of Gear Transmission System with Pitting and Cracking Coupling Faults. *Machines*. volume 11, issue 4, MDPI. Available at: https://www.mdpi.com/2075-1702/11/4/500

[13] USER MANUAL KISSSOFT RELEASE 2023 Available at: https://www.kisssoft.com/en/products/technical-description

[14] FENG, M., MA, H., LI, Z., WANG, Q., WEN, B. (2018). An improved analytical method for calculating time-varying mesh stiffness of helical gears. *Meccanica*, volume 53, issue 4, Springer Available at: https://doi.org/10.1007/s11012-017-0746-6

[15] ZHAN, J., FARD, M., JAZAR, R. (2017). A CAD-FEM-QSA integration technique for determining the time-varying meshing stiffness of gear pairs. *Measurement*, volume 100, Elsevier. Available at: https://www.sciencedirect.com/science/article/pii/S0263224116307540

[16] SÁNCHEZ, M. B., PLEGUEZUELOS, M., PEDRERO, J. I. (2017). Approximate equations for the meshing stiffness and the load sharing ratio of spur gears including hertzian effects. *Mechanism and Machine Theory*, volume 109, Elsevier, pp. 231 – 249. Available at: https://www.sciencedirect.com/science/article/pii/S0094114X16302877

[17] RAGHUWANSHI, N. K., PAREY, A. (2015). Mesh stiffness measurement of cracked spur gear by photoelasticity technique. *Measurement*, volume 73, Elsevier, pp. 439 – 452. Available at: https://doi.org/10.1016/j.measurement.2015.05.035

[18] RAGHUWANSHI, N. K., PAREY, A. (2017). Experimental measurement of spur gear mesh stiffness using digital image correlation technique. *Measurement*, volume 111, Elsevier, pp. 93 – 104. Available at: https://doi.org/10.1016/j.measurement.2017.07.034

[19] RAGHUWANSHI, N. K., PAREY, A. (2018). Experimental measurement of mesh stiffness by laser displacement sensor technique. *Measurement*, volume 128, Elsevier, pp. 63 – 70. Available at: https://doi.org/10.1016/j.measurement.2018.06.035

[20] RAGHUWANSHI, N. K., PAREY, A. (2019). A New Technique of Gear Mesh Stiffness Measurement Using Experimental Modal Analysis. *Journal of Vibration and Acoustics*, volume 141, ASME. Available at: https://doi.org/10.1115/1.4042100

[21] KARPAT, F., YUCE, C., DOĞAN, O. (2020). Experimental measurement and numerical validation of single tooth stiffness for involute spur gears. *Measurement*, volume 150, Elsevier, Available at: https://doi.org/10.1016/j.measurement.2019.107043

[22] KONG, Y., JIANG, H., DONG, N., SHANG, J., YU, P., LI, J., YU, M., CHEN, L. (2023). Analysis of Time-Varying Mesh Stiffness and Dynamic Response of Gear Transmission System with Pitting and Cracking Coupling Faults. *Machines*, volume 11, issue 500, MDPI, Available at: https://doi.org/10.3390/machines11040500